Papers

Sea surface temperature retrieval from MSG/SEVIRI data in the Baltic Sea area

OCEANOLOGIA, 52 (3), 2010.
pp. 331–344.

© *2010, by Institute of Oceanology PAS.*

KEYWORDS
Sea surface temperature
Baltic
Meteosat

Monika Woźniak
Adam Krężel*

Institute of Oceanography,
University of Gdańsk,
al. Marszałka Piłsudskiego 46, PL–81–378 Gdynia, Poland;

e-mail: oceak@univ.gda.pl

*corresponding author

Received 12 November 2009, revised 6 July 2010, accepted 30 July 2010.

Abstract

The aim of the paper was to confirm the proposition that the classical SST algorithms MCSST and NLSST originally prepared for AVHRR data could also be used for Meteosat/SEVIRI data with satisfactory accuracy in the mid-latitude region, where the spatial resolution is about 7×7 km. The research was performed in the southern Baltic Sea (between 13°E 53°N and 21°E 58°N). Data were collected in all the seasons of 2007. The coefficients were found by means of regression analysis. SSTs determined on the basis of AVHRR data were used in the regression analysis instead of in situ data. A set of paired AVHRR and SEVIRI images spaced no more than 8 minutes apart were compared. The results show that the method is capable of producing sea surface temperatures with a statistical error (standard deviation) of 1°C.

1. Introduction

Sea surface temperature (SST) is one of the most important variables in the study of the marine environment: it is, for instance, an indicator of climate change and is used to investigate upper ocean processes and ocean-atmosphere heat exchange. To date, with the exception of traditional in

The complete text of the paper is available at http://www.iopan.gda.pl/oceanologia/

situ measurements performed with buoys, ships etc., global observations of this parameter have been carried out mainly with IR and passive microwave radiometers working on boards of polar-orbiting satellites (Table 1). The drawbacks of the former are the low time resolution, irregularity of measurements and the need for cloudless weather. In the case of the latter cloudiness is not important, but the low spatial resolution limits the area of investigation in practice to open ocean areas. The launching in 2002 of a new generation of geostationary satellites (MSG – Meteosat Second Generation) created the opportunity to increase the time resolution of observations to every 15 minutes. In comparison to its predecessors, Meteosat-8 (since 2008, Meteosat 9), a geostationary satellite, enables SST to be calculated with a much higher time frequency, better spatial resolution and instrumental accuracy. These satellites are equipped with a Spinning Enhanced Visible and Infrared Radiometer Instrument (SEVIRI) with twelve spectral bands. Providing images every 15 minutes (Romaguera et al. 2006), MSG/SEVIRI allows the short-time variability of SST to be observed. The IR 10.8 and 12 μm spectral bands (the 9th and 10th channels of SEVIRI) are used to retrieve SST. This problem has already been discussed in a number of papers. The SST split-window algorithm was analysed using the synergy between MSG and NOAA satellites – this research was carried out with scenes centred on the Iberian Peninsula and the western Mediterranean Sea (Veliente et al. 2007). An investigation on operational SST retrieval from MSG/SEVIRI data over the Atlantic and the western Indian Ocean has been carried out as well. An algorithm was derived from a comparison of satellite data with in situ data and validated by comparison of the SST values obtained with other satellite data sources (Borgne et al. 2006). Romaguera

Table 1. Overview of the present-day sources of satellite SST observations in Europe; IR = infrared, MW = microwave

Instrument	Satellite	Spatial resolution	Temporal resolution	Observing techniques	Expected error, in standard deviation [°C]
AATSR	ENVISAT	1 km	once every 2–3 days	IR	0.3
AVHRR	NOAA	1 km	twice daily	IR	0.5
AMSR-E	Aqua	25 km	daily	MW	0.7
TMI	TRMM	25 km	twice daily	MW	0.7
MODIS	Aqua	1 km	daily	IR	0.7
SEVIRI	Meteosat-9	5 km	every 15 minutes	IR	0.8

et al. (2006) estimated SST from SEVIRI data by testing the algorithm and comparing it with AVHRR products in the case of six test regions for SEVIRI viewing angles of 25°, 30°, 35°, 40°, 45° and 55°. These authors also used the NLSST algorithm, but the coefficients they obtained are inappropriate for the Baltic Sea, as the statistical error (standard deviation) is about 2°C.

This article assesses the possible analogous retrieval of SST from SEVIRI data for the southern Baltic Sea. The problem, however, is that this region is situated close to the range of visualization where the sensing condition is much worse (Figure 1). A further aim of this work is to demonstrate the utility of applying SEVIRI data with a high time resolution to the Baltic Sea region.

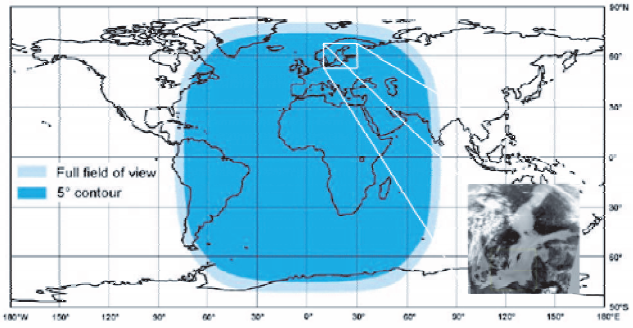

Figure 1. Range of visibility of Meteosat and the study area

2. Material and methods

2.1. Method

SST from AVHRR data is received by the algorithms utilizing IR channel data. The algorithms are definite and used in the ASDIK program created by the Institute of Oceanography, University of Gdańsk.

A SEVIRI has 12 spectral channels (Table 2). Some of them are new, whereas others have already undergone extensive testing as part of AVHRR on board of the NOAA's polar-orbiting satellites (Levizzani et al. 2001). The two infrared channels 10.8 and 12 μm used to calculate SST are nearly the same in the SEVIRI and AVHRR radiometers.

The estimation of SST is based on two classical (Walton et al. 1998, Li et al. 2001) algorithms: Non Linear Sea Surface Temperature (NLSST) and Multichannel Sea Surface Temperature (MCSST) applying the 9th and 10th SEVIRI channels:

Table 2. Spectral channel characteristics of SEVIRI and AVHRR in terms of central, minimum and maximum wavelength of the channels and the main application areas of each channel (Schmetz et al. 2002)

Channel no.	Spectral band [μm]	Spectral band characteristics [μm]					Main observational application
		SEVIRI			AVHRR		
		λ_{cen}	λ_{min}	λ_{max}	λ_{min}	λ_{max}	
1	VIS 0.6	0.635	0.56	0.71	0.58	0.68	surface, clouds, wind fields
2	VIS 0.8	0.81	0.74	0.88	0.72	1.00	surface, clouds, wind fields
3	NIR 1.6	1.64	1.50	1.78	1.58	1.64	surface, cloud phase
4/3b	IR 3.9	3.90	3.48	4.36	3.55	3.93	surface, clouds, wind fields
5	WV 6.2	6.25	5.35	7.15			water vapour, high level clouds, atmospheric instability
6	WV 7.3	7.35	6.85	7.85			water vapour, atmospheric instability
7	IR 8.7	8.70	8.30	9.1			surface, clouds, atmospheric instability
8	IR 9.7	9.66	9.38	9.94			ozone
9/42	IR 10.8	10.80	9.80	11.80	10.3	11.3	surface, clouds, wind fields, atmospheric instability
10/52	IR 12.0	12.00	11.00	13.00	11.5	12.5	surface, clouds, atmospheric instability
11	IR 13.4	13.40	12.40	14.40			high cirrus clouds, atmospheric instability
12	HRV	broadband (about 0.4–1.1 μm)					surface, clouds

$$\mathrm{NLSST} = a_1 T_{11} + (b_1 \mathrm{MCSST} + c_1 S_\theta)(T_{11} - T_{12}) + d_1, \tag{1}$$

$$\mathrm{MCSST} = a_2 T_{11} + (b_2 + c_2 S_\theta)(T_{11} - T_{12}) + d_2, \tag{2}$$

where T_{11}, T_{12} are the brightness temperatures in [K] at 10.8 and 12 μm respectively, $S_\theta = \sec\theta - 1$ and θ is the satellite zenith angle (Krężel et al. 2005, Borgne et al. 2006).

These algorithms were originally designed for AVHRR data. To minimize the influence of atmospheric water vapour the NLSST algorithm makes use of the difference between the 11 and 12 μm IR channels. Atmospheric moisture absorbs more infrared radiation within the 12 μm channel than within the 11 μm one, so the difference in the brightness temperature of these channels is related to the water vapour content of the

atmosphere. There is also another algorithm, the Triple Window Equation, but as it operates on data from the 3.9 μm spectral band, it is usable only at night. According to Le Borgne et al. (2006), the results of this algorithm are not significantly better than those obtained with NLSST or MCSST. The Triple Window Equation was therefore not used in this paper.

The formula (eq. (1)) used to calculate SST with AVHRR data was assumed to be accurate. Therefore, instead of in situ data, the SST/AVHRR was used as standard SST in order to obtain the coefficients of equations (1) and (2) for calculating SST on the basis of SEVIRI data. Because of the different spatial resolutions of AVHRR and SEVIRI images, the spatial resolution of one of them had to be changed. At the latitudes of the southern Baltic, 7×7 pixels of AVHRR images were averaged for comparison with one pixel of SEVIRI images. The coefficients a_n, b_n, c_n, d_n, were found by means of the regression analysis. In the case of every image, a cloud mask was prepared to eliminate cloud cover pixels from the calculations.

2.2. Database

In order to find the coefficients of equations (1) and (2), calculations were performed on the basis of data collected in 2007 (Table 3). The AVHRR data taken by NOAA 15, 17 and 18 were obtained by the Institute of Oceanography, University of Gdańsk Satellite Data Receiving Station, and SEVIRI data taken by Meteosat 8 satellite were obtained from the European Organization for the Exploitation of Meteorological Satellites (EUMETSAT). Taking into account the clearest possible (smallest

Table 3. Dates of the images used in the analysis, $\Delta t = \mathrm{GMT}_{\mathrm{AVHRR}} - \mathrm{GMT}_{\mathrm{SEVIRI}}$

Date	Time [GMT]		Δt	Date	Time [GMT]		Δt
	AVHRR	SEVIRI			AVHRR	SEVIRI	
03.01.07	05:08	05:15	−7	15.07.07	14:58	15:00	−2
23.01.07	11:08	11:15	−7	17.07.07	01:20	01:15	5
03.02.07	04:33	04:30	3	05.08.07	01:21	01:15	6
14.03.07	15:29	15:30	−1	10.08.07	12:04	12:00	4
25.03.07	00:50	00:45	5	14.09.07	01:09	01:15	−6
01.04.07	01:19	01:15	4	23.09.07	11:10	11:15	−5
13.04.07	10:47	10:45	2	08.10.07	14:29	14:30	−1
06.05.07	04:38	04:45	−7	16.10.07	04:50	04:45	5
15.05.07	11:59	12:00	−1	02.11.07	10:57	11:00	−3
09.06.07	11:01	11:00	1	28.11.07	04:25	04:30	−5
25.06.07	04:47	04:45	2	02.12.07	00:54	01:00	−6

proportion of clouds) scenes, two images, one diurnal and one nocturnal, were chosen for each month.

A set of paired AVHRR and SEVIRI images (Figure 2) are spaced in time no more than 8 minutes apart. Images were taken from the southern Baltic Sea (between 13°E 53°N and 21°E 58°N). The zenith angle for this region is between 63.06° and 69.15° (1.1–1.21 radians). SEVIRI images from the area of investigation have a spatial resolution of about 7 km, whereas the spatial resolution of AVHRR images is ca 1 km. To compare images with different spatial resolutions it was necessary to resample the AVHRR images to the same spatial resolution as the SEVIRI ones. Both SEVIRI and AVHRR scenes were referenced to the same geographical framework, the Universal Transverse Mercator (33N).

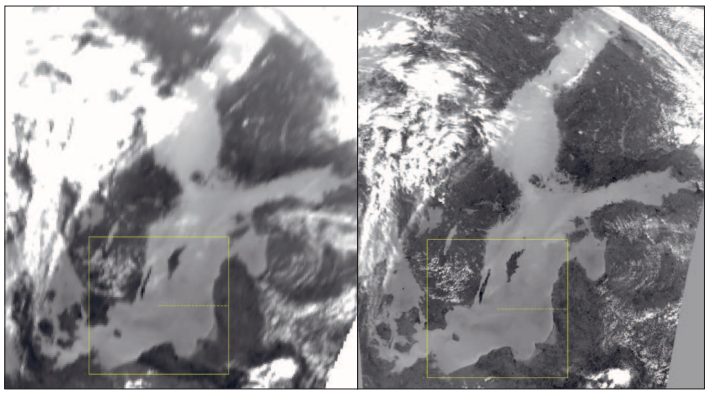

Figure 2. SEVIRI image (left) and AVHRR image (right); the study area is shown

2.3. Cloud masking

A clear cloudless sky is crucial when choosing images for analysis. For the scenes partly covered by clouds, a cloud-mask (Figure 3) was used to eliminate the pixels suspected of being contaminated by clouds or fog. To solve this problem the algorithm proposed by EUMETSAT on the basis of previous papers (Rossow et al. 1985, Saunders & Kriebel 1988, Derrien et al. 1993, Rossow & Gardener 1993a,b, Karlsson 1996, Lutz 1999, Derrien & Le Gléau 2005) with applied local conditions was used to prepare the cloud-mask. This is based on so-called threshold techniques and consists of 7 groups of tests (to detect clouds) (EUMETSAT 2007):

- Group 1: reflectance tests using VIS and near-IR channels.
- Group 2: reflectance difference tests (using all combinations of VIS and near-IR channels).

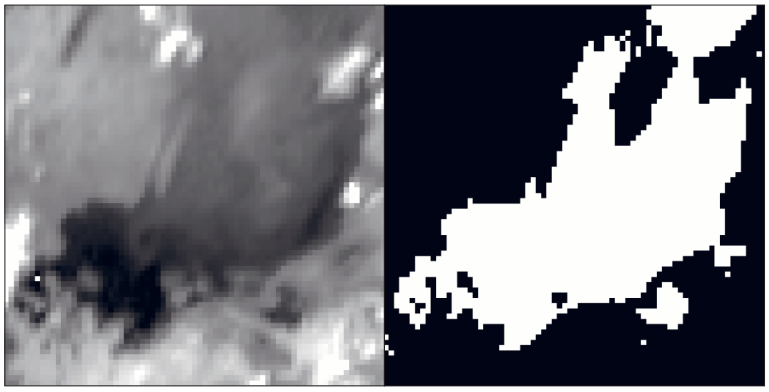

Figure 3. SEVIRI image taken at 05:15 GMT on 03.01.2007 (left). Cloud and land mask (right) – the white area represents the pixels of the cloudless area

- Group 3: temperature tests using the IR window channels.
- Group 4: temperature difference tests (using all combinations of channels 10.8 μm and 12.0 μm with all other IR/WV channels).
- Group 5: standard deviation tests for the window channels on a moving 3×3 pixel target.
- Group 6: snow and ice test.
- Group 7: tests foreseen in the future, e.g. dust storm test, volcanic ash cloud test.

In this work the Group 6 and 7 tests were ignored. With a predefined set of parameters that depend on the viewing geometry/solar zenith angle, the threshold tests themselves can be enabled or disabled. But only the most powerful tests were selected, with the other tests remaining as backup tests. The input data were: SEVIRI reflectance (1st, 2nd and 3rd) channels, brightness temperature (4th, 9th and 10th) channels, the satellite azimuth angle and the solar zenith angle. These tests use a combination of VIS and IR channels and compare the results with determined thresholds (EUMETSAT 2007). If all the tests have been passed we accept the given pixels as representing the sea surface without clouds. The problem is more difficult at night, because only the IR channels can be used then; the cloud-masks obtained at night are thus less reliable. After cloud and land masking only about 30% of the original pixels remain.

3. Results and validation

The coefficients of SST algorithms (eq. (1)) were found by regression analysis (least non-linear squares method); the coefficient of determination

was 95.91%. A data set of cloudless pixels was used. The AVHRR/SST value was the dependent variable (NLSST), the other variables used in the equation were independent variables. Pixels located close to each other have a high autocorrelation coefficient, so to reduce the autocorrelation of the pixels, a random set of 10% of pixels was used for the regression analysis. The sampling was performed ten times and the relevant coefficients were found each time. The result (Table 4) is the mean of 10 trials. SST obtained with the use of these coefficients is given in degrees Celsius.

Table 4. Coefficients of equation (1) obtained for SEVIRI with 95% confidence level ($\alpha = 0.05$)

	$a_{1/2}$	$b_{1/2}$	$c_{1/2}$	$d_{1/2}$
NLSST	0.9962	−0.0019	1.4125	−269.7985
MCSST	0.9960	−0.7936	1.5704	−269.7071

To validate these coefficients another AVHRR and SEVIRI database was prepared. Also, two images – one diurnal and one nocturnal – were taken for each month in 2007 (Table 5). SST calculated from MSG/SEVIRI data using algorithms with the coefficients determined as above was validated by comparison with SST determined from the AVHRR radiometer. For this comparison the relevant error was calculated in accordance with the principle of arithmetic statistics.

Table 5. Dates and times of images taken for validation

Date	Time [GMT]		Date	Time [GMT]	
	AVHRR	SEVIRI		AVHRR	SEVIRI
15.01.07	00:57	01:00	16.07.07	16:14	16:15
27.01.07	10:27	10:30	26.07.07	15:24	15:30
05.03.07	00:50	00:45	05.08.07	11:15	11:15
27.03.07	15:19	15:15	15.08.07	01:18	01:15
01.04.07	11:10	11:15	05.09.07	10:55	11:00
16.04.07	00:22	00:15	25.09.07	00:57	01:00
03.05.07	00:49	00:45	09.10.07	11:45	11:45
04.05.07	15:14	15:15	25.10.07	00:47	00:45
07.06.07	15:04	15:00	17.11.07	15:15	15:15
12.06.07	04:57	05:00	26.12.07	04:57	05:00

Absolute mean error (systematic):

$$< \varepsilon >= N^{-1} \sum_i (\varepsilon_i) \tag{3}$$

Standard deviation (statistical error) of

$$\sigma_\varepsilon = \sqrt{\frac{1}{N}\left(\sum(\varepsilon_i - <\varepsilon>)^2\right)}, \tag{4}$$

where N – number of observations, $\varepsilon_i = (X_{i,\,S} - X_{i,\,A})$, $X_{i,\,S}$ – SEVIRI value, $X_{i,\,A}$ – AVHRR value (the subscript S stands for values calculated from SEVIRI data, A for values from the AVHRR radiometer).

Figure 4 and Table 6 present the result of the validation of the algorithm used to calculate SST in the southern Baltic Sea. The scatter plot illustrates the relationship between the expected and the calculated values. The histogram shows the probability density distribution of the ratio of SST calculated from SEVIRI data to SST determined from the AVHRR radiometer.

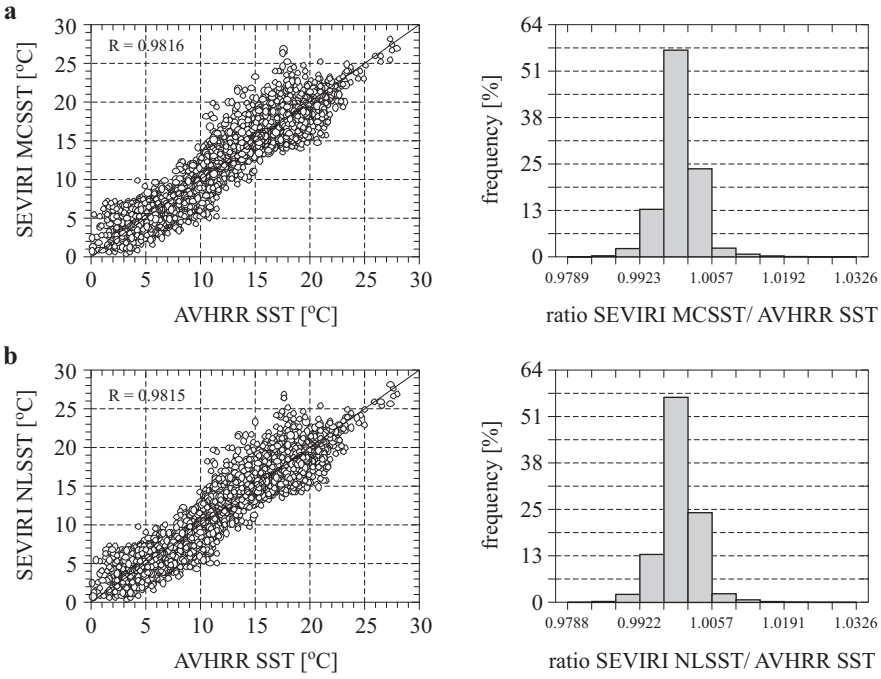

Figure 4. Comparison of sea surface temperature: SST from AVHRR and SST calculated from SEVIRI data; a) MCSST algorithm; b) NLSST algorithm

The level of accuracy seems satisfactory. Discrepancies may be due to the different spatial resolution and the time gaps between the AVHRR and SEVIRI measurement times. The SEVIRI values (pixel size 7×7 km) were compared to the mean value of the corresponding 49 AVHRR pixels.

Table 6. Relative errors in estimating SST from SEVIRI data

Algorithm	No. of data	Arithmetic statistics	
		systematic error $< \varepsilon >$ [°C]	statistical error σ_ε [°C]
MCSST	31408	−0.110032	±1.015481
NLSST	31408	−0.122071	±1.016905

Figure 5 illustrates the statistical characteristics of the calculations. The error of the NLSST algorithm is higher because it contains the error of MCSST as well.

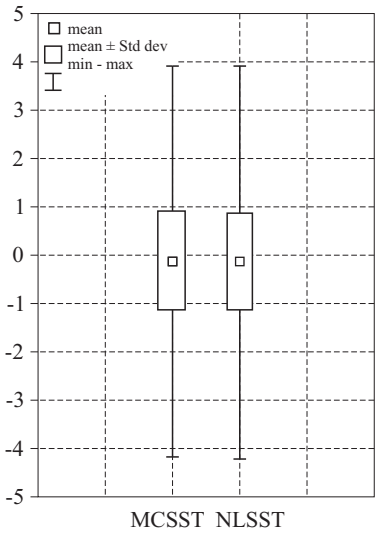

Figure 5. Statistical characteristics of the calculations

4. Applications

MCSST and NLSST algorithms can be used to calculate Sea Surface Temperature in the southern Baltic Sea area from SEVIRI data with satisfactory accuracy, the statistical error being about 1°C.

Because of its high, 15-minute time resolution, the Meteosat-8 (and 9) derived SST products enable short-term processes like coastal upwelling or the spread of river waters in a coastal area to be detected. It can also be used to validate digital models of hydrodynamic and thermal processes.

By way of example, we compared the time variability of SST derived on the basis of AVHRR and SEVIRI data at two localities in the Gulf of Gdańsk – A) 19°28′57″E, 54°36′48″N and B) 19°43′06″E, 54°31′44″N (Figure 6) –

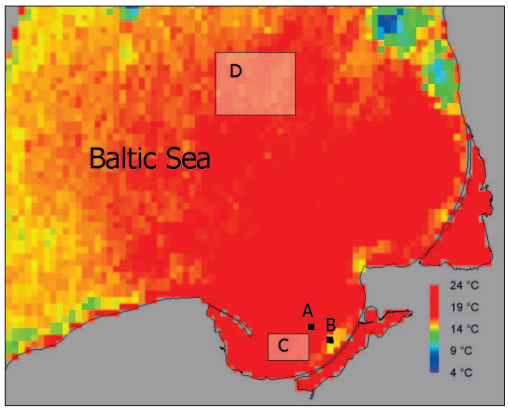

Figure 6. Location of areas (A, B, C and D) chosen for comparison of temporal variability of SST obtained on the basis of SEVIRI data

during a coastal upwelling event. The range of the sea surface temperature in position A (blue curve), i.e. where the upwelled cold water reaches the sea surface, exceeded 3.5°C, whereas at the same time in position B (red curve), the range of values was much lower (Figure 7). We were able to track the details of the spatial and temporal variability of this phenomenon from the beginning to the end.

Another example illustrates the diurnal variability of SST for 25.03.2007 in a 8.6 × 6.3 pixel area in the Gulf of Gdańsk centred at 19°10E 54°40N and in a 15.45 × 12.40 pixel area in the open sea centred at 18°59E 56°02N

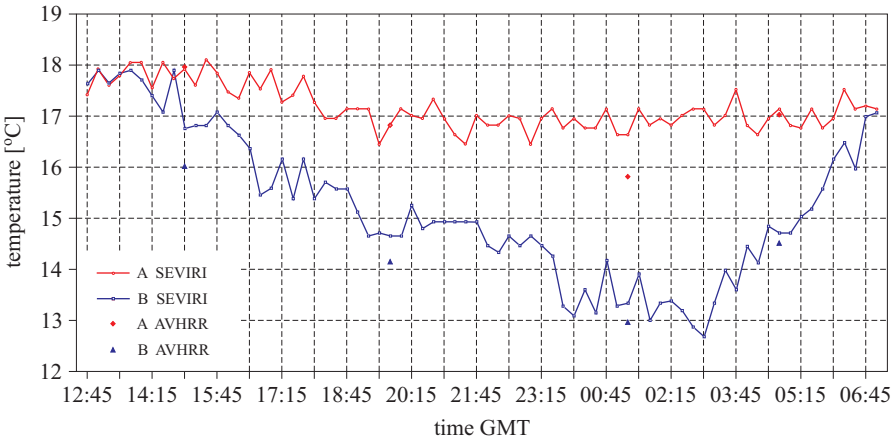

Figure 7. Sea surface temperature [°C] variability at two adjacent sites during a coastal upwelling event in the Gulf of Gdańsk, 7–8.06.2007

(Figure 8). The range of SST from the Gulf of Gdańsk (blue curve) is 0.8°C, apart from a period identified as being covered by clouds (values between 21:00 and 23:00). The minimum temperature of 4.8°C occurred before sunrise at about 03:45 and the maximum of 5.6°C at 13:30. In the open sea area (red curve), the range of values was lower (ca 0.5°C); the minimum temperature was 4.6°C at 02:45 and the maximum 5.2°C at 19:00. For this period only 8 AVHRR measurements were useable. The superiority of SEVIRI derived information over AVHRR in such investigations is therefore evident.

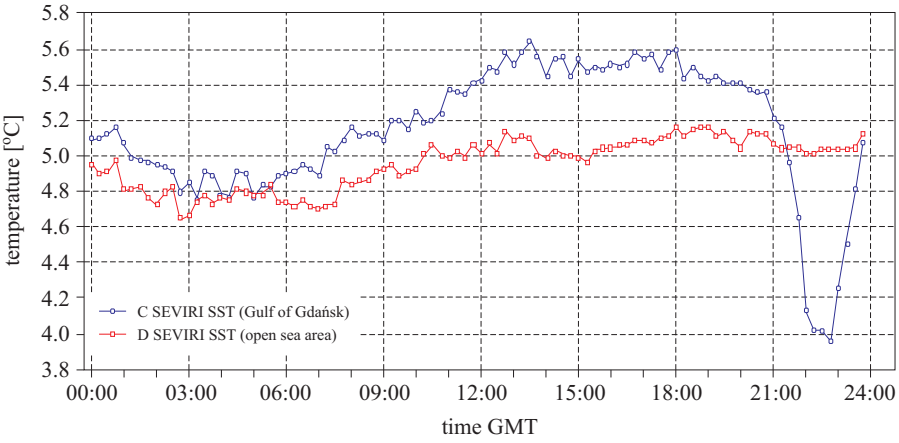

Figure 8. Diurnal variability of SST in areas C (Gulf of Gdańsk) and D (open sea area) on 25.03.2007

5. Conclusions

In this paper two algorithms (equations (1) and (2)) were improved for SEVIRI data in the region of the Baltic Sea. Two IR channels – 10.8 and 12.0 μm – were used. SST obtained from the MCSST and NLSST algorithms were compared with AVHRR data. The algorithms were validated against a database different from that used to obtain it. The statistical error was about 1°C.

The examples show some useful applications of SST derived from SEVIRI data. Despite the comparatively low spatial resolution in comparison to other sources of satellite data, it facilitates the investigation of rapidly changing and very short-term events like coastal upwellings or the post-flood spread of a river, as well as the diurnal variability of SST in different regions of the Baltic Sea.

Acknowledgements

The authors would like to thank EUMETSAT for the MSG/SEVIRI data. Access to Meteosat 8 data was obtained through licence agreement EUM/OPS/LET/06/2277.

References

Borgne P., Legendre G., Marsouin A., 2006, *Operational SST retrieval from MSG/SEVIRI data*, Proc. 2006 EUMETSAT Conf., Helsinki, Finland.

Derrien M., Farki B., Harang L., Le Gléau H., Noyalet A., Pochic D., Sairouni A., 1993, *Automatic cloud detection applied to NOAA-11/AVHRR imagery*, Remote Sens. Environ., 46 (3), 246–267.

Derrien M., Le Gléau H., 2005, *MSG/SEVIRI cloud mask and type from SAFNWC*, Int. J. Remote Sens., 26 (21), 4707–4732.

EUMETSAT, 2007, *Cloud detection for MSG – Algorithm theoretical basis document*, Vol. 2, EUM/MET/REP/07/0132.

Karlsson K.-G., 1996, *Cloud classification with the SCANDIA model*, SMHI Rep. Meteorol. Climatol. No. 67.

Krężel A., Ostrowski M., Szymelfenig M., 2005, *Sea surface temperature distribution during upwelling along the Polish Baltic coast*, Oceanologia, 47 (4), 415–432.

Levizzani V., Schmetz J., Lutz H. J., Kerkmann J., Alberoni P. P., Cervino M., 2001, *Precipitation estimations from geostationary orbit and prospects for METEOSAT Second Generation*, Meteorol. Appl., 8 (1), 23–41.

Li X., Pichel W., Clemente-Colón P., Krasnopolsky V., Sapper J., 2001, *Validation of coastal sea and lake surface temperature measurements derived from NOAA/AVHRR data*, Int. J. Remote Sens., 22 (7), 1285–1303.

Lutz H. J., 1999, *Cloud processing for Meteosat Second Generation*, EUMETSAT Tech. Mem. No. 4.

Romaguera M., Sobrino J. A., Olesen F.-S., 2006, *Estimation of sea surface temperature from SEVIRI data: algorithm testing and comparison with AVHRR products*, Int. J. Remote Sens., 27 (22), 5081–5086.

Rossow W. B., Garder L. C., 1993a, *Cloud detection using satellite measurements of infrared and visible radiances for ISCCP*, J. Climate, 6 (12), 2341–2369.

Rossow W. B., Garder L. C., 1993b, *Validation of ISCCP cloud detections*, J. Climate, 6 (12), 2370–2393.

Rossow W. B., Mosher F., Kinsella E., Arking A., Desbois M., Harrison E., Minnis P., Ruprecht E., Seze G., Simmer C., Smith E., 1985, *ISCCP cloud algorithm intercomparison*, J. Clim. Appl. Meteorol., 24 (9), 877–903.

Saunders R. W., Kriebel K. T., 1988, *An improved method for detecting clear sky and cloudy radiances from AVHRR data*, Int. J. Remote Sens., 9 (1), 123–150.

Schmetz J., Govaerts Y., König M., Lutz H.-J., Ratier A., Tjemkes S., 2002, *A short introduction to Meteosat Second Generation (MSG)*, EUMETSAT.

Valiente J. A., Niclos R., Barbera M. J., Estrela M. J., 2007, *Analysis of the SST Split-Window Equation using the synergy between Meteosat Second Generation and NOAA polar satellites*, Proc. 2007 EUMETSAT Conf., Amsterdam, The Netherlands.

Walton C. C., Pichel W. G., Sapper J. F., May D. A., 1998, *The development and operational application of nonlinear algorithms for the measurement of sea surface temperatures with the NOAA polar-orbiting environmental satellites*, J. Geophys. Res., 103 (C12), 27 999–28 012.